



## Experimental Fock-state bunching capability of non-ideal single-photon states

Petr Zapletal, Tom Darras, Hanna Le Jeannic, Adrien Cavaillès, Giovanni Guccione, Julien Laurat, Radim Filip

### ► To cite this version:

Petr Zapletal, Tom Darras, Hanna Le Jeannic, Adrien Cavaillès, Giovanni Guccione, et al.. Experimental Fock-state bunching capability of non-ideal single-photon states. *Optica*, 2021, 8 (5), pp.743. 10.1364/OPTICA.419230 . hal-03235850

**HAL Id: hal-03235850**

**<https://hal.sorbonne-universite.fr/hal-03235850>**

Submitted on 26 May 2021

**HAL** is a multi-disciplinary open access archive for the deposit and dissemination of scientific research documents, whether they are published or not. The documents may come from teaching and research institutions in France or abroad, or from public or private research centers.

L'archive ouverte pluridisciplinaire **HAL**, est destinée au dépôt et à la diffusion de documents scientifiques de niveau recherche, publiés ou non, émanant des établissements d'enseignement et de recherche français ou étrangers, des laboratoires publics ou privés.



# Experimental Fock-state bunching capability of non-ideal single-photon states

PETR ZAPLETAL,<sup>1,2</sup> TOM DARRAS,<sup>3</sup> HANNA LE JEANNIC,<sup>3,4</sup>  ADRIEN CAVAILLÈS,<sup>3</sup> GIOVANNI GUCCIONE,<sup>3</sup>  JULIEN LAURAT,<sup>3,5</sup> AND RADIM FILIP<sup>1,6</sup>

<sup>1</sup>Department of Optics, Palacký University, 17. listopadu 1192/12, 77146 Olomouc, Czech Republic

<sup>2</sup>Present address: Friedrich-Alexander University Erlangen-Nürnberg (FAU), Department of Physics, 91058 Erlangen, Germany

<sup>3</sup>Laboratoire Kastler Brossel, Sorbonne Université, CNRS, ENS-Université PSL, Collège de France, 4 Place Jussieu, 75005 Paris, France

<sup>4</sup>Present address: Laboratoire Photonique Numérique et Nanoscience, Université de Bordeaux, Institut d'Optique, CNRS, UMR 5298, 33400 Talence, France

<sup>5</sup>e-mail: julien.laurat@sorbonne-universite.fr

<sup>6</sup>e-mail: filip@optics.upol.cz

Received 7 January 2021; revised 30 March 2021; accepted 30 March 2021 (Doc. ID 419230); published 17 May 2021

Advanced quantum technologies, as well as fundamental tests of quantum physics, crucially require the interference of multiple single photons in linear-optics circuits. This interference can result in the bunching of photons into higher Fock states, leading to a complex bosonic behavior. These challenging tasks timely require to develop collective criteria to benchmark many independent initial resources. Here we determine whether  $n$  independent imperfect single photons can ultimately bunch into the Fock state  $|n\rangle$ . We thereby introduce an experimental *Fock-state bunching capability* for single-photon sources, which uses phase-space interference for extreme bunching events as a quantifier. In contrast to autocorrelation functions, this operational approach takes into account not only residual multi-photon components but also a vacuum admixture and the dispersion of individual photon statistics. We apply this approach to high-purity single photons generated from an optical parametric oscillator and show that they can lead to a Fock-state capability of at least 14. Our work demonstrates a novel collective benchmark for single-photon sources and their use in subsequent stringent applications. © 2021 Optical Society of America under the terms of the [OSA Open Access Publishing Agreement](#)

<https://doi.org/10.1364/OPTICA.419230>

## 1. INTRODUCTION

Beyond its fundamental significance, the Hong–Ou–Mandel (HOM) effect [1], where two single photons interfere on a beam splitter, has been central to the development of quantum technologies. With the advance of complex quantum information protocols and networking architectures [2,3], the availability of multiple indistinguishable photons is becoming a cornerstone. Multi-photon interference is required in quantum processing with optical [4–14] or microwave photons [15–17], ranging from boson sampling studies to quantum state engineering. It also plays a key role in quantum sensing [18–20], noiseless amplification [21], quantum key distribution [22,23], and error correction [24–26].

Multi-photon interference leads to a non-trivial redistribution of photons between optical modes. To achieve such interferences, all photons have to be indistinguishable. Several methods have been recently developed to investigate this indistinguishability using different benchmarks, e.g., fidelity [27] or specific photon correlation measures [28–32]. However, the joint impact of photon statistics from many imperfect single-photon states, i.e., exhibiting unwanted vacuum and residual multi-photon components, on multi-photon interference has remained elusive. The joint statistical influence of these parameters cannot be described by evaluating properties of single-photon states that are

averaged over many experimental runs. Hence, we need criteria, experimental data, and subsequent analysis to determine whether independently generated single photons can, in principle, produce the targeted multi-photon interference effects.

Multi-photon interference effects come in a variety of flavors. An extreme event corresponds to the bunching of  $n$  single photons into the Fock state  $|n\rangle$  [33–35]. Such bunching can appear in a linear-optics network with inputs fed by indistinguishable single photons, as shown in Fig. 1. The elementary example is the appearance of the Fock state  $|2\rangle$  based on the HOM effect, as demonstrated in experiments with optical photons and also with microwave photons [16,36], phonons in trapped ions [37], or surface plasmons [38,39]. This extreme bunching event, i.e., the result of a clear operational procedure, enables to introduce a strong benchmark for single-photon states that evaluates their ability to undergo multi-photon interference [40]. This *Fock-state bunching capability* relies on negativities of the resulting Wigner function that provide a very sensitive signature of the non-classicality of the generated higher Fock states [41,42].

In contrast to the well-known second-order autocorrelation function at zero time delay  $g^{(2)}(0)$ , which measures the suppression of the multi-photon contribution and affects the interference visibility [43], the capability is also strongly dependent on the

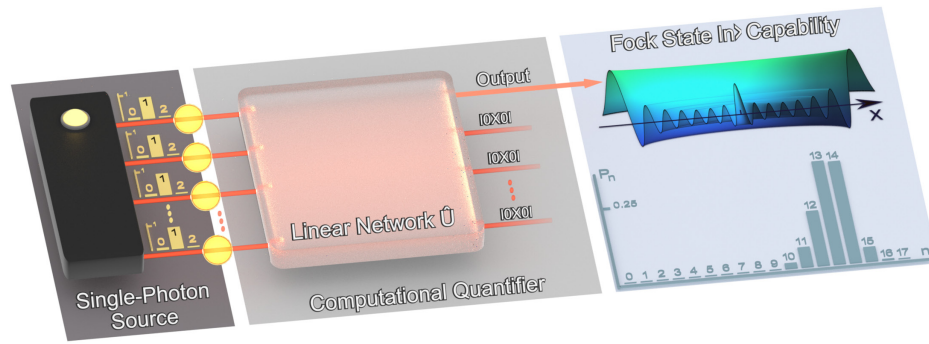


**Fig. 1.** Fock-state bunching capability of non-ideal single-photon states. A single-photon source provides photons with different vacuum admixture and residual multi-photon components, as depicted by the photon-number distributions (left). These states are used as inputs of a balanced linear-optics network  $\hat{U}$ . In an extreme case, all photons can bunch into just one output mode, whereas all other modes are in the vacuum state. This stage is done computationally and provides the expected photon-number distribution  $P_n$  for the output mode (right). The negativities of the associated Wigner function are used to determine the Fock-state capability. In contrast to other measures, this collective benchmark depends not only on the vacuum admixture and multiple-photon statistics of the imperfect input photons, but also on the small discrepancies between them.

vacuum admixture. Another crucial difference is that it collectively tests multiple photon statistics and determines the joint statistical impact of small discrepancies between them. This provides more stringent and accurate evaluation than other available characteristics.

The previous theoretical study based on Monte Carlo simulations has only predicted that the bunching of single photons is affected by vacuum and multi-photon contributions [40]. However, these contributions and their dispersion in non-ideal photon statistics of many independent copies are too complex to be described, specifically when the number of photons increases. Experimental data are necessary to confirm this prediction. Here, we employ the bunching capability to collectively benchmark experimental single-photon states using heralded single photons generated by parametric down-conversion from an optical parametric oscillator (OPO). By tuning the photon source properties, we address the scaling of the capability with the statistics of non-ideal single photons. We hereby provide a crucial insight into the combined effects of non-ideal photon statistics of independently generated single photons. We demonstrate that experimentally generated single photons can bunch into the Fock state  $|14\rangle$  with high fidelity and suppressed higher Fock state contributions. We show that the Fock state capability nonlinearly decreases with photon loss, providing a more stringent characterization than  $g^{(2)}(0)$ , which is independent of photon loss, and also more than the negative Wigner function that decreases only linearly. Our results indicate that despite the negative impact of multi-photon contributions typically reported using  $g^{(2)}(0)$ , they prevent the bunching of single-photon states into a respective Fock state less severely than optical loss.

## 2. QUANTIFIER PRINCIPLE

We first describe the quantifier principle. To collectively test the ability of the generated single photons to undergo multi-photon interference, we computationally determine the Wigner function of the higher Fock state, which can, in principle, appear from multiple copies of the single-photon state, as depicted in Fig. 1. The area in phase space, where the Wigner function of the ideal Fock state  $|n\rangle$  is negative, is composed of  $n/2$  or  $(n-1)/2$  concentric annuli if  $n$  is an even number or an odd number, respectively.

By definition, a single-photon state has the capability of the Fock state  $|n\rangle$  if the Wigner function of the state, which can be generated from  $n$  independent copies of the single-photon state, has the same number of negative annuli as the ideal Fock state  $|n\rangle$  [40]. The negative annuli in the Wigner function witness the non-classical nature of multi-photon interference in phase space. The Fock-state capability, which is determined computationally, collectively tests the copies of a single-photon state, even though any multi-copy procedure is not implemented in the laboratory.

In theory,  $n$  copies of the ideal single-photon state  $|1\rangle$  have the capability of an arbitrary Fock state  $|n\rangle$ . For states generated by single-photon sources, the negative annuli in the Wigner function are sensitive to the presence of vacuum and multi-photon contributions. Also, the exact distribution of residual multi-photon statistics in many non-ideal single-photon states is not known. As a consequence, the joint effect of small discrepancies between individual single-photon copies on multi-photon interference has to be investigated by applying the quantifier on photon statistics measured in an experiment. In this way, we can determine whether the single-photon sources are of sufficient quality for applications in quantum technology that require multi-photon interference.

## 3. SINGLE-PHOTON GENERATION AND MULTIPLE DATA SETS

To study this benchmark, we used heralded single-photon states generated using a two-mode squeezer, i.e., a type-II phase-matched OPO operated well below threshold (see Supplement 1). The signal and idler photons at 1064 nm are separated on a polarizing beam splitter, and the idler photon is detected via a high-efficiency superconducting nanowire single-photon detector. This detection event heralds the generation of a single photon in the signal mode. The generated state is emitted into a well-defined spatiotemporal mode [44], with a bandwidth of about 65 MHz. The state is measured via high-efficiency homodyne detection, with visibility of the interference with the local oscillator above 99%, and reconstructed via maximum-likelihood algorithms [45]. The experimental setup has been described elsewhere [46,47].

Importantly, the OPO used in this work exhibits a close-to-unity escape efficiency, i.e., the transmission of the output coupler is much larger than the intracavity losses [48]. As a result, a large

**Table 1. Photon-Number Statistics of Heralded Single Photons<sup>a</sup>**

	$P_1$	$P_{2+}$	$g^{(2)}(0)$	$2\pi \times W(0, 0)$
1	$0.53 \pm 0.01$	$0.010 \pm 0.006$	$0.07 \pm 0.05$	$-(0.05 \pm 0.02)$
2	$0.62 \pm 0.02$	$0.013 \pm 0.008$	$0.07 \pm 0.04$	$-(0.23 \pm 0.03)$
3	$0.74 \pm 0.01$	$0.016 \pm 0.008$	$0.06 \pm 0.03$	$-(0.47 \pm 0.02)$
4	$0.72 \pm 0.01$	$0.05 \pm 0.01$	$0.2 \pm 0.04$	$-(0.45 \pm 0.02)$
5	$0.83 \pm 0.01$	$0.07 \pm 0.01$	$0.2 \pm 0.03$	$-(0.67 \pm 0.02)$
6	$0.86 \pm 0.01$	$0.02 \pm 0.01$	$0.05 \pm 0.03$	$-(0.73 \pm 0.02)$
7	$0.91 \pm 0.01$	$0.02 \pm 0.01$	$0.05 \pm 0.02$	$-(0.82 \pm 0.02)$

<sup>a</sup>Each set is obtained by successive measurements under the same conditions (in particular, pump power). The table displays the single-photon component  $P_1$ , multi-photon probability  $P_{2+}$ , second-order correlation function  $g^{(2)}(0)$ , and negativity at the origin of the Wigner function.

heralding efficiency can be obtained, i.e., a very low admixture of vacuum. A single-photon component up to 91% is achieved. Also, by changing the pump power, the multi-photon component can be increased at will. These features enable us to explore different combinations of state imperfections. Seven sets of data were recorded, each of them obtained by a repetitive measurement of single-photon states generated under the same conditions. Parameters of the sets are given in Table 1. They include the single-photon component  $P_1$  and the probability  $P_{2+}$  of finding two or more photons. These measured quantities also give access to the conditional second-order autocorrelation function at zero-time delay  $g^{(2)}(0)$  [47].

#### 4. EXPERIMENTAL FOCK-STATE BUNCHING CAPABILITY

To test a particular data set for the Fock-state capability  $n$ , the data are randomly partitioned into  $n$  subsets from which  $n$  photon-number statistics are obtained and used as the quantifier inputs. The output-state Wigner function of the computational quantifier is averaged over 30 such random choices. From the averaged output-state Wigner function, it is determined whether the data set has Fock-state capability  $n$  (see Supplement 1). The capability for all data sets is depicted in Fig. 2 as a function of  $P_1$  and  $P_{2+}$ . The quantifier is presently computationally limited by Fock-state capability 14 (see Supplement 1), which is already a very large number in this operational context. All data sets for which this capability 14 is obtained may also have the capability of a higher Fock state. In the following, we describe the different measured points and typical trends.

First, single-photon states with a low purity due to a vacuum component close to 50% (brown bars in Fig. 2, sets 1 and 2 in Table 1) have only the trivial capability of Fock state |1>, despite their very low  $g^{(2)}(0)$ . This shows that the broadly used autocorrelation function does not fully characterize the ability to bunch into higher Fock states exhibiting non-classical signatures. In particular, this example demonstrates that the capability is more sensitive to vacuum mixture, as a state obtained from two copies of these single photons would have a positive Wigner function. Due to their trivial capability, such states are not a useful resource for the preparation of large Fock states that could be used, e.g., for quantum metrology [18–20] or error correction [24–26].

The necessary condition for a non-trivial capability  $n > 1$  is to reach a single-photon component  $P_1 > 2/3$  [40]. Above this threshold, the capability moderately grows with  $P_1$ . As can be seen in Fig. 2, the state corresponding to the green bar (set 3 in Table 1)

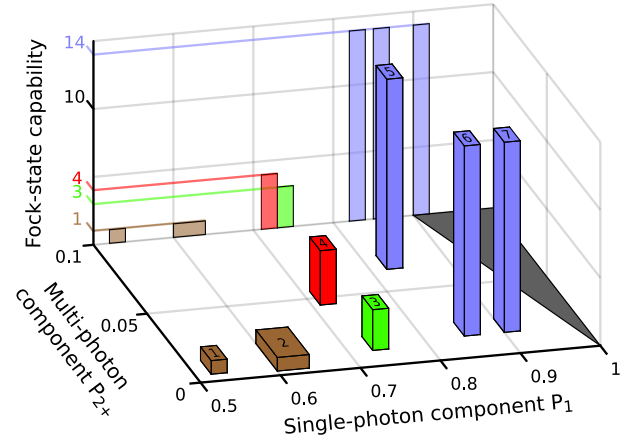


**Fig. 2.** Fock-state bunching capability of the experimentally generated single-photon states. The capability is given as a function of the single-photon component  $P_1$  and of the multi-photon probability  $P_{2+}$  for the different sets given in Table 1. These parameters are averaged over photon-number statistics from a given data set obtained by successive measurements under the same experimental conditions. Colors denote the Fock-state capability. The gray-shaded area excludes the unphysical probabilities  $P_1 + P_{2+} > 1$ . The standard deviation of the probabilities are given by the thicknesses of the color bars.

has a multi-photon component  $P_{2+} = 0.02$  and the capability of Fock state |3>. The state associated with the red bar (set 4) has the capability of Fock state |4> despite having a similar single-photon component as the previous state but a larger, still low, probability  $P_{2+} = 0.05$ . For a given  $P_1$ , an increase in  $P_{2+}$  may thereby lead to a larger capability. Actually, this increase in  $P_{2+}$  comes in that case with a decrease in the vacuum component, indicating that the bunching is less affected by multi-photon contributions than a vacuum admixture. We have shown in additional simulations that at a fixed vacuum contribution, the capability decreases with the multi-photon component.

Finally, for  $P_1 > 0.8$ , the capability is expected to rapidly increase and to diverge at  $P_1^{(\infty)} = 0.885$ , where an arbitrary capability can be reached [40]. The experimental results agree well with this prediction and highlight the nonlinearity of the quantifier. The verification of this trend is an important benchmark for the development of single-photon sources. The data sets indicated with blue bars have at least capability 14. For set 7, note that its  $g^{(2)}(0) = 0.05$  does not significantly differ from that of the states with the trivial Fock-state capability. A capability of 14 is also achieved for lower single-photon fidelities  $P_1$  and higher multi-photon contributions  $P_{2+}$ , even for a state with four times larger  $g^{(2)}(0) = 0.2$ . However, these states might have a lower capability than set 7 due to the saturation to 14 because of computational power.

#### 5. DISCUSSION: EFFECT OF LOSS AND TRUNCATION

Figure 3 presents the output of the computational quantifier with 14 input states randomly chosen from data set 7, i.e., the set with the highest heralding efficiency and lowest multi-photon component. Figure 3(a) first provides the cut through the Wigner function. The output Wigner function is fitted by the one of a lossy Fock state |14>, with a fitted attenuation parameter  $\eta = 0.9205 \pm 0.0005$ . The fit shows that the oscillations of the



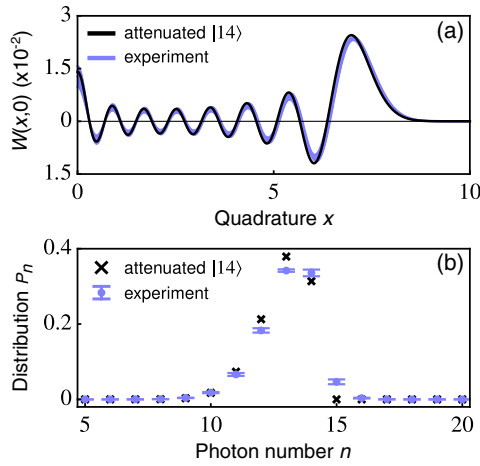


**Fig. 3.** Quantifier output. (a) Cut through the output Wigner function of the computational quantifier with 14 experimental photon-number statistics as inputs. The line thickness provides the  $3\sigma$  interval for the values of the Wigner function. The black fit corresponds to the attenuated Fock state  $|14\rangle$  with an attenuation  $\eta = 0.9205$ . (b) Associated photon-number distribution (blue points) compared to the one of the attenuated Fock state  $|14\rangle$  (black crosses). The output Wigner function and the photon-number distribution are averaged over 30 random choices of photon-number statistics from data set 7, with  $P_1 = 0.91$  and  $P_{2+} = 0.02$ .

output Wigner function in phase space coincide with the ones of the attenuated Fock state  $|14\rangle$ . The photon-number statistics of the output state and attenuated Fock state are compared in Fig. 3(b). The good cutoff of the multi-photon contributions with more than 14 photons in the statistics of the output state is another feature that further demonstrates the high quality of the initial single-photon states. Such a result was made possible only for single-photon states with limited multi-photon contributions and a very low vacuum admixture, as provided by the OPO-based source used in this work.

We now come to an additional characterization of the quantifier, i.e., its evolution with optical losses. This quantifier *depth*, in analogy to non-classicality depth [49], is tested by considering attenuation for two states randomly chosen from different data sets. Figure 4 shows the Fock-state capability as a function of the attenuation parameter  $\eta$ , for the state with  $P_1 = 0.91$  and  $P_2 = 0.02$  (blue in Fig. 2) and the state with  $P_1 = 0.72$  and

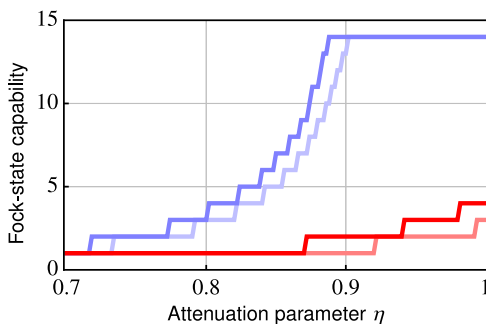


**Fig. 4.** Fock-state bunching capability and optical loss. The blue and red lines provide the Fock-state capability for a single random choice of  $n$  attenuated photon-number statistics obtained from data sets 7 and 4, with a capability of 14 and 4, respectively. These capabilities are compared to the capabilities of truncated states, i.e., with neglected multi-photon contributions (light blue and light red lines).

$P_2 = 0.05$  (red in Fig. 2). Both states exhibit a low  $g^{(2)}(0)$  parameter (which is preserved with attenuation), but different initial capabilities 14 and 4, respectively. As can be seen, the capability depends nonlinearly on the attenuation  $\eta$ . This is in contrast to the negativity of the single-photon Wigner function, which decreases linearly with attenuation. As a result, the capability allows more sensitive benchmarking of single-photon states than the negativity of the Wigner function.

The results in Fig. 4 are also superimposed with two plots that give the evolution of the capability with optical losses for states whose photon-number statistics are truncated, i.e., neglecting the multi-photon contribution. The discrepancy in the Fock-state capability between the experimental states and the truncated ones demonstrates that the multi-photon contributions play a significant role in such bunching experiments. The truncation of multi-photon contributions can be a limiting approximation when multi-photon interference is involved.

## 6. CONCLUSION

In conclusion, with the advance of quantum technologies, novel procedures and applications put challenging demands on resources and required benchmarking [50]. In this broad context of utmost importance, we have employed the *Fock-state bunching capability* to collectively benchmark experimental single-photon states for the first time. We have investigated the behavior of this test with photon statistics and loss. This quantifier, which is highly nonlinear, has a clear operational meaning in terms of photon merging and moreover takes into account the unavoidable dispersion of individual copies of single-photon states.

Due to high-purity states based on a state-of-the-art OPO, this work has experimentally verified the numerically predicted threshold,  $P_1 > 0.885$ , to observe a large Fock-state capability. A capability of at least 14 has been demonstrated due to the very low two-photon component and the large heralding efficiency. Importantly, we have shown that the capability is more sensitive to optical losses than the single-photon negativity of the Wigner function and fidelity. Based on our numerical data, we also deduced that a moderate increase in the ratio of the multi-photon contributions to the vacuum does not decrease the capability. This shows that despite the negative impact of multi-photon contributions, they prevent the bunching of single-photon states into a single Fock state less severely than optical losses.

In the present implementation, we have estimated photon-number distributions from homodyne detection. Multiplexed single-photon detectors [51,52] or photon-number resolving superconducting detectors [53–55] should enable a direct measurement of the Fock-state bunching capability. Also, this benchmark does not depend on the nature of the source and can thereby be used to characterize microwave photons in superconducting circuits [15], plasmons at metal–dielectric surfaces [38,39], phonons in trapped-ion [56] or optomechanics experiments [57], and collective excitations in atomic ensembles [58–60]. Finally, the multi-photon interference quantifier can be modified to investigate the capability of other resource states, e.g. squeezed states or Schrödinger cat states [13,61], to produce different target states such as NOON states [18–20] or superpositions of squeezed states (GKP states) [62], opening a new avenue for testing the potential of light emitters for advanced quantum state engineering.

**Funding.** Horizon 2020 Framework Programme (FET proactive HOT 732894, FETFLAG Quantum Internet Alliance 820445, Marie Curie Fellowship HELIOS IF-749213, QuantERA ERA-NET ShoQC 731473, Twinning project NonGauss 951737); MEYS project 8C20002; Grantová Agentura České Republiky (20-16577S); Agence Nationale de la Recherche (HyLight project ANR-17-CE30-0006); DIM Ile-de-France Sirteq (PhD Fellowship).

**Acknowledgment.** The authors thank K. Huang and O. Morin for their contributions in the early stage of the experiment. R.F. acknowledges Czech Science Foundation and national funding from the MEYS. G.G. acknowledges support by the European Union and P.Z. by the European Union's Horizon 2020 Research and Innovation Framework Programme. T.D. acknowledges a Ph.D. Fellowship from DIM Ile-de-France Sirteq.

**Disclosures.** The authors declare no conflicts of interest.

**Data Availability.** Data underlying the results presented in this paper are not publicly available at this time but may be obtained from the authors upon reasonable request.

**Supplemental document.** See [Supplement 1](#) for supporting content.

## REFERENCES

- C. K. Hong, Z. Y. Ou, and L. Mandel, "Measurement of subpicosecond time intervals between two photons by interference," *Phys. Rev. Lett.* **59**, 2044–2046 (1987).
- I. A. Walmsley, "Quantum optics: science and technology in a new light," *Science* **348**, 525–530 (2015).
- F. Flamini, N. Spagnolo, and F. Sciarrino, "Photonic quantum information processing: a review," *Rep. Prog. Phys.* **82**, 016001 (2019).
- A. Peruzzo, M. Lobino, J. C. F. Matthews, N. Matsuda, A. Politi, K. Poulios, X.-Q. Zhou, Y. Lahini, N. Ismail, K. Wörhoff, Y. Bromberg, Y. Silberberg, M. G. Thompson, and J. L. O'Brien, "Quantum walks of correlated photons," *Science* **329**, 1500–1503 (2010).
- A. Crespi, R. Osellame, R. Ramponi, V. Giovannetti, R. Fazio, L. Sansoni, F. De Nicola, F. Sciarrino, and P. Mataloni, "Anderson localization of entangled photons in an integrated quantum walk," *Nat. Photonics* **7**, 322–328 (2013).
- M. Tillmann, B. Dakic, R. Heilmann, S. Nolte, A. Szameit, and P. Walther, "Experimental boson sampling," *Nat. Photonics* **7**, 540–544 (2013).
- M. A. Broome, A. Fedrizzi, S. Rahimi-Keshari, J. Dove, S. Aaronson, T. C. Ralph, and A. G. White, "Photonic boson sampling in a tunable circuit," *Science* **339**, 794–798 (2013).
- J. B. Spring, B. J. Metcalfe, P. C. Humphreys, W. S. Kolthammer, X.-M. Jin, M. Barbieri, A. Datta, N. Thomas-Peter, N. K. Langford, D. Kundys, J. C. Gates, B. J. Smith, P. G. R. Smith, and I. A. Walmsley, "Boson sampling on a photonic chip," *Science* **339**, 798–801 (2013).
- N. Spagnolo, C. Vitelli, M. Bentivegna, D. J. Brod, A. Crespi, F. Flamini, S. Giacomini, G. Milani, R. Ramponi, P. Mataloni, R. Osellame, E. F. Galvão, and F. Sciarrino, "Experimental validation of photonic boson sampling," *Nat. Photonics* **8**, 615–620 (2014).
- M. Bentivegna, N. Spagnolo, C. Vitelli, F. Flamini, N. Viggianiello, L. Latmiral, P. Mataloni, D. J. Brod, E. F. Galvão, A. Crespi, R. Ramponi, R. Osellame, and F. Sciarrino, "Experimental scattershot boson sampling," *Sci. Adv.* **1**, e1400255 (2015).
- H. Wang, Y. He, Y.-H. Li, Z.-E. Su, B. Li, H.-L. Huang, X. Ding, M.-C. Chen, C. Liu, J. Qin, J.-P. Li, Y.-M. He, C. Schneider, M. Kamp, C.-Z. Peng, S. Höfling, C.-Y. Lu, and J.-W. Pan, "High-efficiency multiphoton boson sampling," *Nat. Photonics* **11**, 361–365 (2017).
- H.-S. Zhong, Y. Li, W. Li, L.-C. Peng, Z.-E. Su, Y. Hu, Y.-M. He, X. Ding, W. Zhang, H. Li, L. Zhang, Z. Wang, L. You, X.-L. Wang, X. Jiang, L. Li, Y.-A. Chen, N.-L. Liu, C.-Y. Lu, and J.-W. Pan, "12-photon entanglement and scalable scattershot boson sampling with optimal entangled-photon pairs from parametric down-conversion," *Phys. Rev. Lett.* **121**, 250505 (2018).
- P. Minzioni, C. Lacava, T. Tanabe, J. Dong, X. Hu, G. Csaba, W. Porod, G. Singh, A. E. Willner, A. Alaiman, V. Torres-Company, J. Schröder, A. C. Peacock, M. J. Strain, F. Parmigiani, G. Contestabile, D. Marpaung, Z. Liu, J. E. Bowers, L. Chang, S. Fabbri, M. R. Vázquez, V. Bharadwaj, S. M. Eaton, P. Lodahl, X. Zhang, B. J. Eggleton, W. J. Munro, K. Nemoto, O. Morin, J. Laurat, and J. Nunn, "Roadmap on all-optical processing," *J. Opt.* **21**, 063001 (2019).
- G. Guccione, T. Darras, H. Le Jeannic, V. B. Verma, S. W. Nam, A. Cavallès, and J. Laurat, "Connecting heterogeneous quantum networks by hybrid entanglement swapping," *Sci. Adv.* **6**, eaba4508 (2020).
- W. Pfaff, C. J. Axline, L. D. Burkhardt, U. Vool, P. Reinhold, L. Frunzio, L. Jiang, M. H. Devoret, and R. J. Schoelkopf, "Controlled release of multiphoton quantum states from a microwave cavity memory," *Nat. Phys.* **13**, 882–887 (2017).
- Y. Y. Gao, B. J. Lester, Y. Zhang, C. Wang, S. Rosenblum, L. Frunzio, L. Jiang, S. M. Girvin, and R. J. Schoelkopf, "Programmable interference between two microwave quantum memories," *Phys. Rev. X* **8**, 021073 (2018).
- B. Peropadre, G. G. Guerreschi, J. Huh, and A. Aspuru-Guzik, "Proposal for microwave boson sampling," *Phys. Rev. Lett.* **117**, 140505 (2016).
- J. C. F. Matthews, X. Q. Zhou, H. Cable, P. J. Shadbolt, D. J. Saunders, G. A. Durkin, G. J. Pryde, and J. L. O'Brien, "Towards practical quantum metrology with photon counting," *npj Quantum Inf.* **2**, 16023 (2016).
- A. E. Ulanov, I. A. Fedorov, D. Sychev, P. Grangier, and A. I. Lvovsky, "Loss-tolerant state engineering for quantum-enhanced metrology via the reverse Hong-Ou-Mandel effect," *Nat. Commun.* **7**, 11925 (2016).
- S. Slussarenko, M. M. Weston, H. M. Chrzanowski, L. K. Shalm, V. B. Verma, S. W. Nam, and G. J. Pryde, "Unconditional violation of the shot-noise limit in photonic quantum metrology," *Nat. Photonics* **11**, 700–703 (2017).
- T. C. Ralph and A. P. Lund, "Nondeterministic noiseless linear amplification of quantum systems," *AIP Conf. Proc.* **1110**, 155–160 (2009).
- M. Ghalaii, C. Ottaviani, R. Kumar, S. Pirandola, and M. Razavi, "Long-distance continuous-variable quantum key distribution with quantum scissors," *IEEE J. Sel. Top. Quantum Electron.* **26**, 6400212 (2020).
- M. Ghalaii, C. Ottaviani, R. Kumar, S. Pirandola, and M. Razavi, "Discrete-modulation continuous-variable quantum key distribution enhanced by quantum scissors," *IEEE J. Sel. Areas Commun.* **38**, 506–516 (2020).
- M. H. Michael, M. Silveri, R. T. Brierley, V. V. Albert, J. Salmilehto, L. Jiang, and S. M. Girvin, "New class of quantum error-correcting codes for a bosonic mode," *Phys. Rev. X* **6**, 031006 (2016).
- B. Bergmann and P. van Loock, "Quantum error correction against photon loss using NOON states," *Phys. Rev. A* **94**, 012311 (2016).
- L. Hu, Y. Ma, W. Cai, X. Mu, Y. Xu, W. Wang, Y. Wu, H. Wang, Y. P. Song, C.-L. Zou, S. M. Girvin, L.-M. Duan, and L. Sun, "Quantum error correction and universal gate set operation on a binomial bosonic logical qubit," *Nat. Phys.* **15**, 503–508 (2019).
- L. Aolita, C. Gogolin, M. Kliesch, and J. Eisert, "Reliable quantum certification of photonic state preparations," *Nat. Commun.* **6**, 8498 (2015).
- A. Crespi, R. Osellame, R. Ramponi, M. Bentivegna, F. Flamini, N. Spagnolo, N. Viggianiello, L. Innocenti, P. Mataloni, and F. Sciarrino, "Suppression law of quantum states in a 3D photonic fast Fourier transform chip," *Nat. Commun.* **7**, 10469 (2016).
- N. Viggianiello, F. Flamini, L. Innocenti, D. Cozzolino, M. Bentivegna, N. Spagnolo, A. Crespi, D. J. Brod, E. F. Galvão, R. Osellame, and F. Sciarrino, "Experimental generalized quantum suppression law in Sylvester interferometers," *New J. Phys.* **20**, 033017 (2018).
- T. Giordani, F. Flamini, M. Pompili, N. Viggianiello, N. Spagnolo, A. Crespi, R. Osellame, N. Wiebe, M. Walschaers, A. Buchleitner, and F. Sciarrino, "Experimental statistical signature of many-body quantum interference," *Nat. Photonics* **12**, 173–178 (2018).
- D. J. Brod, F. Galvão, N. Viggianiello, F. Flamini, N. Spagnolo, and F. Sciarrino, "Witnessing genuine multiphoton indistinguishability," *Phys. Rev. Lett.* **122**, 063602 (2019).
- F. Flamini, M. Walschaers, N. Spagnolo, N. Wiebe, A. Buchleitner, and F. Sciarrino, "Validating multi-photon quantum interference with finite data," *Quantum Sci. Technol.* **5**, 045005 (2020).
- O. Steuernagel, "Synthesis of Fock states via beam splitters," *Opt. Commun.* **138**, 71–74 (1997).
- B. M. Escher, A. T. Avelar, and B. Baseia, "Synthesis of arbitrary Fock states via conditional measurements on beam splitters," *Phys. Rev. A* **72**, 045803 (2005).
- K. R. Motes, R. L. Mann, J. P. Olson, N. M. Studer, E. A. Bergeron, A. Gilchrist, J. P. Dowling, D. W. Berry, and P. P. Rohde, "Efficient recycling strategies for preparing large Fock states from single-photon sources: applications to quantum metrology," *Phys. Rev. A* **94**, 012344 (2016).
- C. Lang, C. Eichler, L. Steffen, J. M. Fink, M. J. Woolley, A. Blais, and A. Wallraff, "Correlations, indistinguishability and entanglement in Hong-Ou-Mandel experiments at microwave frequencies," *Nat. Phys.* **9**, 345–348 (2013).

37. K. Toyoda, R. Hiji, A. Noguchi, and S. Urabe, "Hong-Ou-Mandel interference of two phonons in trapped ions," *Nature* **527**, 74–77 (2015).
38. R. W. Heeres, L. P. Kouwenhoven, and V. Zwiller, "Quantum interference in plasmonic circuits," *Nat. Nanotechnol.* **8**, 719–722 (2013).
39. J. S. Fakonas, H. Lee, Y. A. Kelaita, and H. A. Atwater, "Two-plasmon quantum interference," *Nat. Photonics* **8**, 317–320 (2014).
40. P. Zapetal and R. Filip, "Multi-copy quantifiers for single-photon states," *Sci. Rep.* **7**, 1484 (2017).
41. W. Schleich, *Quantum Optics in Phase Space* (Wiley, 2001).
42. S. Haroche and J. M. Raimond, *Exploring the Quantum: Atoms, Cavities, and Photons* (Oxford University, 2006).
43. H. Ollivier, S. E. Thomas, S. C. Wein, I. M. de Buy Wenniger, N. Coste, J. C. Lored, N. Somaschi, A. Harouri, A. Lemaitre, I. Sagnes, L. Lanco, C. Simon, C. Anton, O. Krebs, and P. Senellart, "Hong-Ou-Mandel interferences with imperfect single photon sources," *Phys. Rev. Lett.* **126**, 063602 (2021).
44. O. Morin, C. Fabre, and J. Laurat, "Experimentally accessing the optimal temporal mode of traveling quantum light states," *Phys. Rev. Lett.* **111**, 213602 (2013).
45. A. I. Lvovsky and M. G. Raymer, "Continuous-variable optical quantum state tomography," *Rev. Mod. Phys.* **81**, 299–332 (2009).
46. O. Morin, J. D. Bancal, M. Ho, P. Sekatski, V. D'Auria, N. Gisin, J. Laurat, and N. Sangouard, "Witnessing trustworthy single-photon entanglement with local homodyne measurements," *Phys. Rev. Lett.* **110**, 130401 (2013).
47. H. Le Jeannic, V. B. Verma, A. Cavaillès, F. Marsili, M. D. Shaw, K. Huang, O. Morin, S. W. Nam, and J. Laurat, "High-efficiency WSi superconducting nanowire single-photon detectors for quantum state engineering in the near infrared," *Opt. Lett.* **41**, 5341–5344 (2016).
48. O. Morin, J. Liu, K. Huang, F. Barbosa, C. Fabre, and J. Laurat, "Quantum state engineering of light with continuous-wave optical parametric oscillators," *J. Vis. Exp.* **87**, e51224 (2014).
49. C. T. Lee, "Measure of the nonclassicality of nonclassical states," *Phys. Rev. A* **44**, R2775 (1991).
50. J. Eisert, D. Hangleiter, N. Walk, I. Roth, D. Markham, R. Parekh, U. Chabaud, and E. Kashefi, "Quantum certification and benchmarking," *Nat. Rev. Phys.* **2**, 382–390 (2020).
51. G. Harder, Ch. Silberhorn, J. Rehacek, Z. Hradil, L. Motka, B. Stoklasa, and L. L. Sánchez-Soto, "Local sampling of the Wigner function at telecom wavelength with loss-tolerant detection of photon statistics," *Phys. Rev. Lett.* **116**, 133601 (2016).
52. M. Bohmann, J. Tiedau, T. Bartley, J. Sperling, Ch. Silberhorn, and W. Vogel, "Incomplete detection of nonclassical phase-space distributions," *Phys. Rev. Lett.* **120**, 063607 (2018).
53. G. Harder, T. J. Bartley, A. E. Lita, S. W. Nam, T. Gerrits, and Ch. Silberhorn, "Single-mode parametric-down-conversion states with 50 photons as a source for mesoscopic quantum optics," *Phys. Rev. Lett.* **116**, 143601 (2016).
54. M. Klass, E. Schlottmann, H. Flayac, F. P. Laussy, F. Gericke, M. Schmidt, M. V. Helversen, J. Beyer, S. Brodbeck, H. Suchomel, S. Höfling, S. Reitzenstein, and C. Schneider, "Photon-number-resolved measurement of an exciton-polariton condensate," *Phys. Rev. Lett.* **121**, 047401 (2018).
55. J. Tiedau, T. J. Bartley, G. Harder, A. E. Lita, S. W. Nam, T. Gerrits, and Ch. Silberhorn, "Scalability of parametric down-conversion for generating higher-order Fock states," *Phys. Rev. A* **100**, 041802 (2019).
56. D. Kienzler, H.-Y. Lo, V. Negevitsky, C. Flümman, M. Marinelli, and J. P. Home, "Quantum harmonic oscillators state control in a squeezed fock basis," *Phys. Rev. Lett.* **119**, 033602 (2017).
57. S. Hong, R. Riedinger, I. Marinković, A. Wallucks, S. G. Hofer, R. A. Norte, M. Aspelmeyer, and S. Gröblacher, "Hanbury Brown and Twiss interferometry of single phonons from an optomechanical resonator," *Science* **358**, 203–206 (2017).
58. J. Laurat, H. de Riedmatten, D. Felinto, C.-W. Chou, E. W. Schomburg, and H. J. Kimble, "Efficient retrieval of a single excitation stored in an atomic ensemble," *Opt. Express* **14**, 6912–6918 (2006).
59. E. Bimbard, R. Boddada, N. Vitrant, A. Grankin, V. Parigi, J. Stanojevic, A. Ourjoumtsev, and P. Grangie, "Homodyne tomography of a single photon retrieved on demand from a cavity-enhanced cold atom memory," *Phys. Rev. Lett.* **112**, 033601 (2014).
60. N. V. Corzo, J. Raskop, A. Chandra, A. S. Sheremet, B. Gouraud, and J. Laurat, "Waveguide-coupled single collective excitation of atomic arrays," *Nature* **566**, 359–362 (2019).
61. D. V. Sychev, A. E. Ulanov, A. A. Pushkina, M. W. Richards, I. A. Fedorov, and A. I. Lvovsky, "Enlargement of optical Schrödinger's cat states," *Nat. Photonics* **11**, 379–382 (2017).
62. D. Gottesman, A. Kitaev, and J. Preskill, "Encoding a qubit in an oscillator," *Phys. Rev. A* **64**, 012310 (2001).